A novel method to quantify atmospheric stability

Svenningsen, Lasse; Slot, René M.M.; Thøgersen, Morten L.

Published in:
Journal of Physics: Conference Series

DOI (link to publication from Publisher):
10.1088/1742-6596/1102/1/012009

Publication date:
2018

Document Version
Publisher's PDF, also known as Version of record

A novel method to quantify atmospheric stability

IOP Conf. Series: Journal of Physics: Conf. Series **1102** (2018) 012009 doi:10.1088/1742-6596/1102/1/012009

A novel method to quantify atmospheric stability

Lasse Svenningsen[1], René M. M. Slot[1,2], and Morten L. Thøgersen[1]

[1]EMD International A/S, Niels Jernes Vej 10, Aalborg, Denmark
[2]Aalborg University, Dep. of Civ. Eng., Thomas Manns Vej 23, Aalborg, Denmark

E-mail: ls@emd.dk

Summary. Atmospheric stability significantly influences the characteristics of a wind resource and strongly affects wind turbine power production and structural loads. Stability is governed by the thermal structure of the atmospheric boundary layer (ABL). Unstable ABLs are convective and increase turbulence, but reduce vertical wind shear, while stable ABLs reduce turbulence and increase wind shear. In neutral ABLs mechanical effects of terrain and roughness dominate.

The Monin-Obukhov length (MOL) and Richardson numbers are the recommended methods to quantify atmospheric stability. These methods require advanced and expensive measurements of temperature differences or 3D-sonic covariances, not installed on standard wind power masts.

This study presents a novel methodology to quantify stability based only on standard wind measurements. At high wind speeds turbulence and wind shear converge to the neutral ABL response in a given direction while the relative deviations of shear and turbulence at lower wind speeds strongly correlate with stability. When normalized by the neutral shear and turbulence, these deviations directly quantify stability. Here we present a novel method to estimate MOL directly from the ratio of normalized shear and turbulence.

The proposed method to quantify stability from standard wind measurements, provides an important input to advanced wind flow modelling of stability effects to improve the accuracy of predicted power production and structural loads.

1. Introduction - Importance and effects of atmospheric stability

Atmospheric stability is fundamental to understanding and characterizing the wind climate at a potential wind farm location as it significantly influences the wind turbine power production [1,2] and the structural loads [3–5]. Stability is determined by the buoyancy forces in the atmospheric boundary layer (ABL) and, hence, the acceleration or attenuation of vertical air movements. These buoyancy effects lead to convective mixing in the unstable ABL (UABL) or attenuation of vertical movements and stratification in the stable ABL (SABL). In the UABL turbulence is increased above the background level determined by the mechanical effects of terrain and roughness and the convective mixing reduces the vertical variation of wind speed (i.e. wind shear). The SABL has the opposite effect on wind shear and turbulence, and reduces turbulence to below the mechanical level resulting in stratified flow and increased wind shear. The neutral ABL (NABL) has neutral buoyancy and the wind flow is dominated by the mechanical effects of surface terrain and roughness.

The well-established standard methods to quantify atmospheric stability are based on measurements of vertical temperature differences or turbulent fluxes estimated from 3D-sonic covariance measurements. These methods are the Richardson numbers Ri (gradient or bulk) and the Monin-Obukhov length (MOL) L, typically given as $1/L$ [2,3,6]. Ri and $1/L$ estimate the ratio of buoyancy

effects and mechanical effects and tend to zero in the NABL, where mechanical effects dominate. Both Ri and $1/L$ are negative in UABLs and positive in SABLs.

Alternative methods have been proposed to categorize stability directly from wind shear [7]. Such methods neglect the important effect that shear is not only controlled by stability, but to a large degree also by terrain and roughness. Neglecting these effects leads to wrong stability classification in directions with very high or low surface roughness or significant terrain-induced wind speed-up.

In this paper we present a novel method to quantify stability based on measurements from a standard mast setup typical for wind power projects. Such a mast only logs 10min mean and st. dev. of wind speed, and 10min wind direction mean at multiple measuring heights (z). This setup allows calculation of the 10min values of the wind shear exponent, $\alpha(t)$, and turbulence intensity, $TI(t) = \sigma(t)/u(t)$, which both depend strongly on stability. Section 2 describes the theoretical basis of the proposed method. Section 3 presents the four steps of the method and section 4 demonstrates the application of the method to observations from the Cabauw tower. Section 5 analyses the validity of the main assumption of the proposed method.

2. Monin-Obukhov similarity theory for shear and turbulence

The Monin-Obukhov Similarity Theory (MOST) provides a theoretical basis to quantify the expected deviations of wind shear as a function of stability, i.e. MOL. MOST is valid in the surface layer where fluxes are close to constant, typically covering the lower 10% of the ABL or approximately up to 50-100m above ground level [8,9]. The basic governing equation is the logarithmic wind profile with the MOST stability correction, Ψ_m.

$$u(z) = \frac{u_*}{\kappa}\left\{\ln\left(\frac{z}{z_0}\right) - \Psi_m\left(\frac{z}{L}\right)\right\} \quad (1)$$

Ψ_m is an integral of the non-dimensional wind shear function, φ_m, which is the 'universal scaling function' for momentum [8,9]. u_* is the friction velocity, κ is Von Karman's constant typically taken to be 0.4, z is the height above ground, and z_0 is the roughness length. In the limit of neutral stability $\varphi_m = 1$, and $\Psi_m = 0$. The vertical wind shear exponent, α, is typically estimated using multiple heights on the wind profile, but may also be calculated directly from the wind speed derivative at a single height using the non-dimensional wind shear function, φ_m, according to [4]:

$$\alpha \equiv \frac{du/dz}{u/z} = \frac{u_*}{u\cdot\kappa}\varphi_m\left(\frac{z}{L}\right) \quad (2)$$

The longitudinal component of turbulence ($\sigma_u = TI \cdot u$) does not fully follow the universal scaling laws of MOST as it does not entirely scale with height. However, σ_u does scale with u_* and depend on L, and non-dimensional scaling functions, φ_1, have been published in [8,10] covering the stable and unstable side, respectively. In the neutral limit φ_1 approaches a constant value. On the stable side φ_1 depends on z/L [11,12], whereas on the unstable side φ_1 depends only on $1/L$ and slightly on the boundary layer depth, z_i [8,10,13,14] as summarized in equations (3) and (4).

$$\sigma_u = u_*\varphi_1\left(\frac{z}{L}\right) \quad \text{(stable)} \quad (3)$$

$$\sigma_u = u_*\varphi_1\left(\frac{z_i}{L}\right) \quad \text{(unstable)} \quad (4)$$

The typical theoretical expressions published for Ψ_m, φ_m and φ_1 are summarized in Table 1 with the relevant references. The constants a, b and c are general and vary across the φ-functions and stability categories in the table. However, in the cited references the typical values for Ψ_m are b=4.7 (or 5.0) for stable conditions and b=16 for unstable conditions where c=1/4. Similarly, b=4.7 for φ_m under stable conditions and b=16, c=-1/4 for unstable conditions. For φ_1 a=1.7, b=0.31, c=0.63 under stable conditions and a=2.3, b=0.042, c=1/3 for unstable.

The phi-functions must be continuous across the stability spectrum, hence, their stable and unstable expressions must tend to the same neutral limit for large L. This is automatically fulfilled for φ_m as the

published expressions are 'pre-normalized' to unity in the neutral limit. For φ_1 this continuity requires the constant a to be identical across the neutral, stable and unstable categories, but published values vary in the range of 1.7-2.5 [8,11]. For the purpose of this study we use the typical and intermediate value a=2.3 from [10]. As we shall see later the proposed method will only utilize ratios of φ_1, so the assumed value of a has limited significance except to ensure continuity across the stability categories.

Table 1. *Summary of published expressions for the universal functions, Ψ_m, φ_m and φ_1, under neutral, stable and unstable conditions. Relevant references are placed besides each expression. The constants for the neutral limit may be inferred from letting $|L| \to \infty$.*

	Neutral	Stable		Unstable	
$\boldsymbol{\Psi_m}$	0	$-b\frac{z}{L}$	[8,10]	$\ln\left[\left(\frac{1+x^2}{2}\right)\left(\frac{1+x}{2}\right)^2\right] - 2\tan^{-1}(x) + \frac{\pi}{2}$ $x = \left(1 - b\frac{z}{L}\right)^c$	[8,10]
$\boldsymbol{\varphi_m}$	1	$1 + b\frac{z}{L}$	[8–10]	$\left(1 - b\frac{z}{L}\right)^c$	[8–10]
$\boldsymbol{\varphi_1}$	a	$a + b\left(\frac{z}{L}\right)^c$	[11,12]	$a\left(1 - b\frac{z_i}{L}\right)^c$	[10,13]

MOST makes several assumptions about the characteristics of the surface layer and their validity influences the accuracy of the presented method. In addition to constant fluxes, MOST assumes horizontal homogeneity e.g. of terrain and roughness as well as quasi-stationary conditions [9]. Additionally, according to [8] MOST is not valid at low wind speeds. For wind power applications the latter is not a problem as wind turbines do not operate below 3-5m/s. The other MOST assumptions are neither fulfilled for most real wind turbine locations nor for most 10min intervals during turbine operation. However, as we shall see in the next section describing the method and in section 5 validating the method, these assumptions are partially alleviated by using of ratios of the universal φ-functions. These ratios do not require MOST to be accurate in an absolute sense, only in a relative sense, to accurately predict the stability induced deviations of shear and turbulence from their neutral level.

3. Description of the proposed method

A typical wind power mast setup with wind speed and direction measurements at multiple levels, allows calculation of 10min values of the wind shear exponent, $\alpha(t)$, and turbulence intensity, $TI(t)$. The proposed method seeks to quantify stability in each 10min data interval via quantifying the deviations of shear and turbulence from their neutral levels in the wind direction of each 10min interval. The method has four processing steps to quantify stability in each 10min interval described in the following.

Step 1 *– estimate neutral levels of shear and TI versus direction*

First step of the method is to estimate the neutral levels of turbulence, $\widehat{TI}_N(\theta)$, and wind shear, $\hat{\alpha}_N(\theta)$, as a function of direction. These are estimated from the highest 1-3% of wind speeds using robust median statistics applied to a 10-20° wide rolling window of wind directions ensuring a smooth and robust estimation in 1° direction steps.

Step 2 *– estimate normalized deviations of shear and TI*

Second step is to calculate the normalized shear and turbulence and their deviations from unity ($\delta\alpha$ and δTI) for each 10min measurement. The normalization is relative to the neutral estimates from 'step 1', as shown in equation (5).

$$\delta TI(t) = \frac{TI(t)}{\widehat{TI}_N(\theta)} - 1 \quad \& \quad \delta\alpha(t) = \frac{\alpha(t)}{\hat{\alpha}_N(\theta)} - 1 \tag{5}$$

Step 3 *– apply smoothing kernel to enhance stability signal*
Third step, which can be omitted, is to apply a smoothing kernel to the time series of normalized shear and TI deviations to enhance the stability signal and reduce spurious variations. A centered median filter with a 1-3 hour window is a very effective compromise between retaining the signal and reducing the noise considerably.

Step 4 *– make diagnostic plot and estimate Monin-Obukhov lengths*
In the final step the normalized shear and TI deviations $\{\delta TI(t), \delta\alpha(t)\}$ are used to make a diagnostic plot to visually check the data. In the plot the magnitude of the $\{\delta TI(t), \delta\alpha(t)\}$ deviation represents the strength of the stability effects and the direction indicates the type of stability:

- Neutral: low magnitude, i.e. $\sqrt{\delta TI(t)^2 + \delta\alpha(t)^2} \to 0$
- Stable: significant magnitude in 2. quadrant, $\delta TI(t) < 0 \;\&\; \delta\alpha(t) > 0$
- Unstable: significant magnitude in 4. quadrant, $\delta TI(t) > 0 \;\&\; \delta\alpha(t) < 0$

The normalized shear and TI directly quantify stability and can be converted to an estimate of MOL based on theoretical considerations presented later in this section.

A large magnitude of deviations in the first and third quadrants of the diagnostic plot in 'step 4' can represent more ambiguous stability effects where the data deviate from the basic assumptions. Such data could result from systematic biases in the estimation of the neutral levels at high wind speeds due to complex meteorological effects. Such an effect could be the Charnock effect where roughness increases with wind speed for water surfaces, leading to increasing shear and turbulence in the high wind speed limit, introducing a bias. Similarly, data with significant magnitude in first quadrant ($\delta TI(t) > 0$ & $\delta\alpha(t) > 0$) could result from stable conditions coinciding with a ramp in wind speed or unstable conditions with large scale convective perturbations to the profile. Data in third quadrant ($\delta TI(t) < 0$ & $\delta\alpha(t) < 0$) could result from stable conditions with a shallow nocturnal ABL with measurement heights in the residual layer.

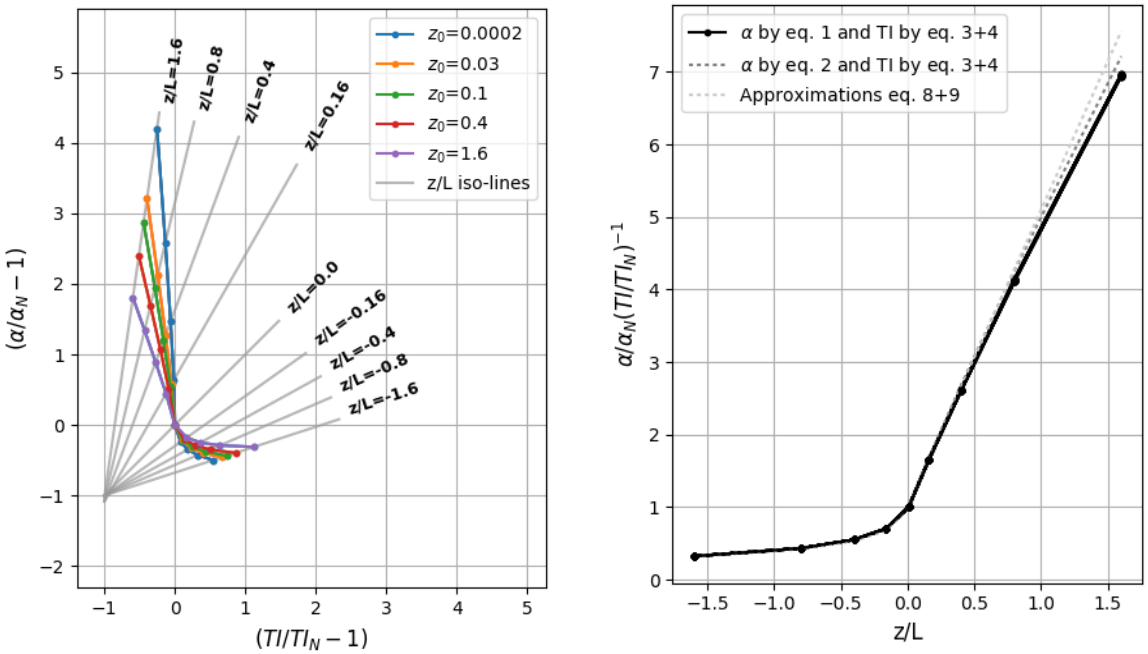

Figure 1. *Left: theoretical normalized shear and turbulence deviations for five roughnesses (coloured lines) and nine stabilities (grey z/L-'iso-lines'). Right: ratios of $\alpha/\alpha_N\,(TI/TI_N)^{-1}$ versus z/L for the same data, where the five roughness curves collapse to a single (black) curve across the stabilities.*

To study the proposed method we generate theoretical wind speed profiles and turbulence data and apply steps 1 and 2 of the proposed method to calculate theoretical normalized deviations of shear and turbulence. The results are shown in Figure 1 (left) and the data are generated using the Ψ_m and φ_1 expressions in Table 1 with the constants outlined above the table, as well as equations (1) and (3)+(4) to calculate the mean wind speed profile and turbulence intensity. These calculations are performed for nine stabilities ranging from very unstable, over neutral to very stable represented by values of L from -50m over ±10,000m to 50m. Height above ground is set to $z = 80\text{m}$ with 40m and 140m included for shear estimation to match the observations presented later in section 4. The ABL height is set to $z_i = 2000\text{m}$, but the results have a very low sensitivity to this assumption. This calculation setup is further repeated for five different roughness values ranging from $2 \cdot 10^{-4}$m to 1.6m. In Figure 1 (left) the solid lines show the normalized shear and turbulence deviations for these five roughness values across the nine stabilities. Points representing same z/L (stability) are connected to form z/L-'iso-lines'. Note that these z/L-'iso-lines' are all straight and converge to the same point {-1,-1}.

The peculiar convergence to {-1,-1} of the z/L-'iso-lines' in Figure 1 (left) indicate that the ratios of the normalized shear and turbulence are independent of roughness. If instead just the normalized shear and turbulence are plotted the z/L-'iso-lines' converge to {0,0}. As a consequence the five curves for different roughnesses collapse to a single curve in Figure 1 (right) when plotting the normalized shear divided by the normalized turbulence versus z/L. This single curve strongly resembles the shape of the universal function for momentum, φ_m, but does not match it exactly. To further analyse this result, equations (2), (3), and (4) are combined to investigate the theoretical expectation for the ratio of the normalized shear and turbulence. It turns out that in this ratio the wind speeds and friction velocities all cancel out as they appear both in equation (2) and equations (3)+(4), hence, yielding the result for a particular z/L:

$$\frac{\alpha}{\alpha_N}\left(\frac{TI}{TI_N}\right)^{-1} = \frac{\varphi_m}{\varphi_{m,N}}\left(\frac{\varphi_1}{\varphi_{1,N}}\right)^{-1} \tag{6}$$

This is a significant result. Not only does the ratio of the normalized shear and turbulence annul the effect of roughness as seen in Figure 1. Equation (6) shows that the ratio of normalized shear and turbulence equals the ratio of the two corresponding universal φ-functions, each normalized to its neutral value. All other constants or variables cancel out. This is important because in the ratios of the φ-functions normalized to its neutral value, the constants in Table 1 to some degree cancel out and become less important – in particularly for turbulence. This increases the general validity of equation (6) with the important example being complex terrain with steep slopes where modified constants for φ_1 are reported in [13]. Their results indicate that the adjustment of φ_1 in steep topography can be treated as factor $f\left(\hat{\theta}, z/L\right)$ as summarized in equation (7), where $\hat{\theta}$ is a characteristic terrain slope in a particular direction.

$$\varphi_{1,topo} \cong f\left(\hat{\theta}, \frac{z}{L}\right)\, \varphi_{1,flat} \tag{7}$$

If $f\left(\hat{\theta}, z/L\right)$ does not depend too strongly on z/L, it will mostly cancel out when φ_1 is normalized to its neutral value (cf. equation 6), making the φ_1 ratios more valid in non-flat topography. These arguments seem plausible also for normalized wind shear, φ_m, for moderate deviations from neutral stability in steep terrain, which also appears to be indicated by the results in [15] for unstable conditions. Similar considerations apply to the bias introduced by a Charnock effect for water surfaces. The increasing water roughness with wind speed will positively bias the neutral estimates of both shear and turbulence, slightly skewing a $\{\delta TI, \delta\alpha\}$ plot like Figure 1 (left), but the bias will, at least partially, cancel out in the estimated ratios $\alpha/\alpha_N\,(TI/TI_N)^{-1}$ damping the effect of the bias.

An important consequence of Figure 1 (right) is that it can be used to estimate L by inversely looking-up values of z/L from observed ratios of $\alpha/\alpha_N\,(TI/TI_N)^{-1}$. Taking a closer look at Figure 1 (right) the stable part is close to linear in z/L and the unstable part is close to linear in $-\ln(-z/L)$. This conclusion

can also be reached by analysing equation (6) inserting the φ-expresssions in Table 1 using the values outlined above the table. The linear and log-linear approximations to the stable and unstable regimes are summarized in equations (8) and (9) and shown in Figure 1 together with the exact model.

$$\text{Stable:} \quad \frac{\alpha}{\alpha_N}\left(\frac{TI}{TI_N}\right)^{-1} > 1, \qquad \frac{\alpha}{\alpha_N}\left(\frac{TI}{TI_N}\right)^{-1} \cong 4.1\frac{z}{L} + 1 \tag{8}$$

$$\text{Unstable:} \quad \frac{\alpha}{\alpha_N}\left(\frac{TI}{TI_N}\right)^{-1} < 1, \qquad \frac{\alpha}{\alpha_N}\left(\frac{TI}{TI_N}\right)^{-1} \cong -0.15\ln\left(\frac{-z}{L}\right) + 0.4 \tag{9}$$

This result derived from equation (6) states that MOL can be estimated directly from measurements of wind speed and turbulence, although MOL itself depends on heat flux. However, the effect of heat flux enters implicitly via the estimation and normalization with the neutral shear and TI levels to quantify the deviations from the neutral state. Hence, this normalization accounts for the effect of non-zero heat flux and non-neutral temperature profile.

4. Demonstration of proposed method at Cabauw tower

The proposed method is demonstrated using data from the Cabauw meteorological research tower [16] situated in quite homogenous terrain in the Netherlands. The mast is equipped with high grade research instruments and the data are carefully filtered for faulty measurements. Wind speed measurements from $z \in \{40\text{m}, 80\text{m}, 140\text{m}\}$ are used for the shear estimates and the 80m data for turbulence and wind directions. Figure 2 shows the result of 'step 1' estimation of the neutral TI and shear levels for the direction 220°±10°. Estimated neutral levels are shown as green lines and the 2% highest wind speeds utilized for the estimation are shown in magenta. The trumpet shape of the data points towards lower wind speeds (grey samples) reflects the increasing importance of stability leading to larger deviations and increased variability around the neutral levels.

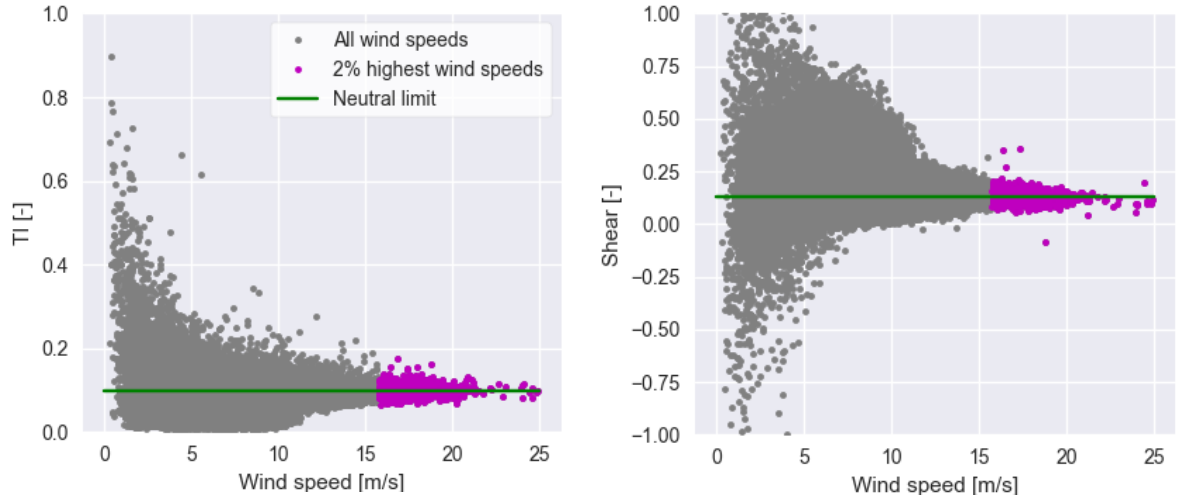

Figure 2. *All TI (left) and shear (right) 10min data for a 20° window around 220°. Values for the 2% highest wind speeds are shown in magenta. Green lines show the 'neutral estimates' of TI and shear.*

Figure 3 shows the result of applying steps 2+3 to estimate the normalized shear and turbulence deviations and how smoothing enhances the stability signal. The plot shows eight days covering the rise and fall of a high wind speed event where both shear and turbulence deviations are close to zero during the highest wind speeds. As the winds level off a clear diurnal stability variation emerges with positive shear deviations and negative TI deviations during night and vice versa during day (vertical grid lines are 00:00h). Note the increased noise of the normalized deviations for wind speeds below 5m/s and note also how the smoothing effectively reduces the spurious high frequency variations.

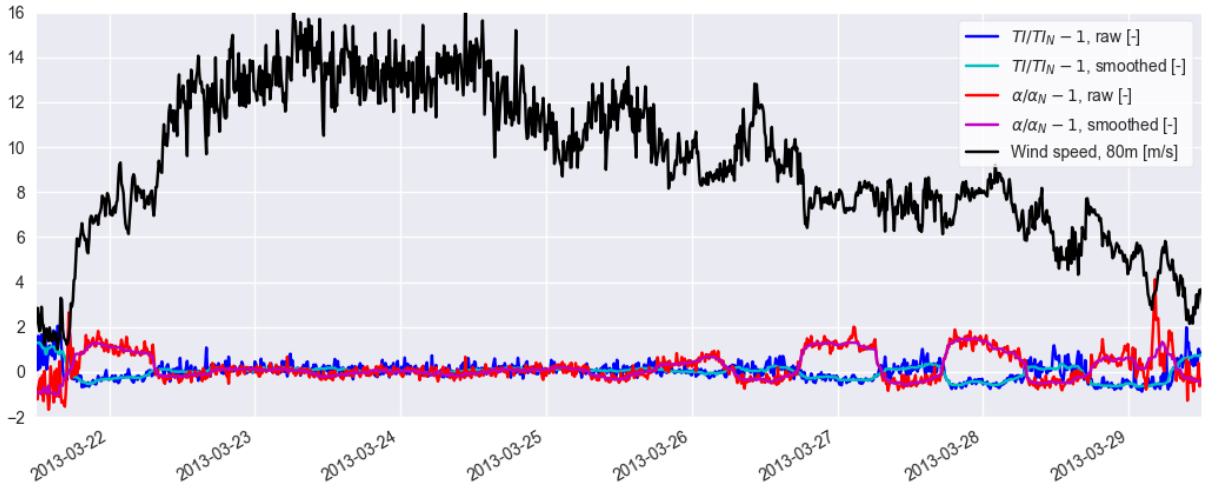

Figure 3. *Estimated normalized shear and turbulence deviations and wind speed at 80m for a period of eight days around a high wind speed event. Smoothed versions of the shear and turbulence deviations are overlaid for comparison of the effect of smoothing.*

Figure 4 shows the final result of steps 1-4 for the Cabauw data plotting the smoothed normalized deviations $\{\delta TI(t), \delta\alpha(t)\}$ for all the data. The colours indicate different wind speed thresholds and the superimposed z/L-'iso-lines' are based on equations (8) and (9). The z/L values are chosen to represent typical L thresholds of different stability regimes [e.g. 6]: neutral ($|z/L| \leq 80\text{m}/500\text{m} = 0.16$), over near neutral ($|z/L| \leq 80\text{m}/200\text{m} = 0.4$) to stable/unstable ($|z/L| \leq 80\text{m}/100\text{m} = 0.8$) and very stable/unstable ($|z/L| \leq 80\text{m}/50\text{m} = 1.6$).

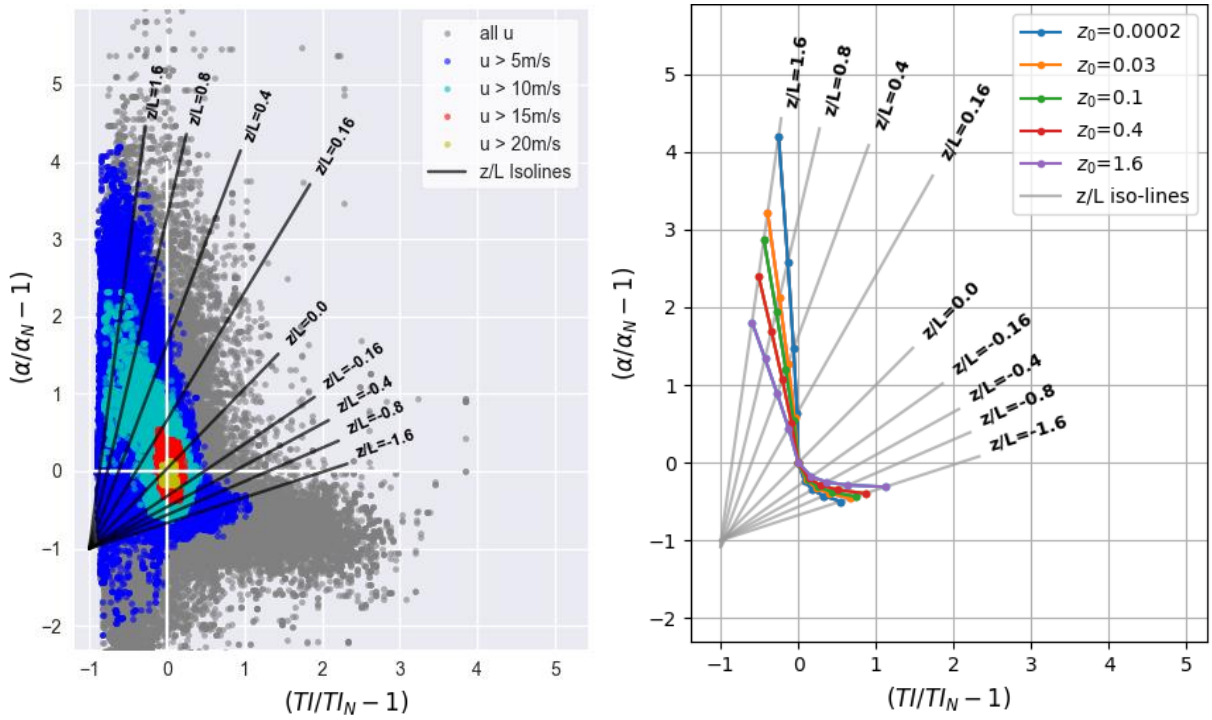

Figure 4. *Left: Estimated $\{\delta TI(t), \delta\alpha(t)\}$ data for Cabauw for different wind speed thresholds clearly showing data gradually moving towards the centre (neutral stability) for higher wind speeds. 'Iso-lines' for z/L from equations (8) and (9) are superimposed. Right: Figure 1 (left) for comparison.*

Notice the clear bulls-eye like centering of the data for the higher wind speed thresholds and how the observed $\{\delta TI(t), \delta\alpha(t)\}$ data resembles the theoretical data in Figure 1, albeit with some scatter. Figure 1 is inserted (right) for easy comparison. The grey data points represent wind speeds below 5m/s where the MOST starts to break down [8] and show a considerably larger scatter than the coloured points at higher wind speed. However, such low wind speeds are not relevant as wind turbines stop below 3-5m/s.

5. Validation of main assumption of the proposed method

The foundation of the proposed method is the existence of the 'universal' relationship illustrated in Figure 1 (right) between MOL and the ratio of normalized shear and normalized TI. This universal relationship is derived in equation (6) as the ratio of MOST universal φ-functions, which are only a function of MOL. Equations (8) and (9) approximate equation (6) for the φ-expressions summarized in Table 1. The existence of this universal relationship can be analysed and validated when concurrent measurements of both MOL and estimates of normalized shear and turbulence are available for a mast. We perform this validation analysis for data from two very diverse research masts both measuring MOL with 3D-sonic equipment. The two masts are high quality research grade masts operated by DTU at the Høvsøre test site [17] on the Danish west coast, and at Ryningsnäs [18] situated in a forest in south-western Sweden. Consistent sensor heights are available for the masts and 80m is used for MOL, wind direction and TI and 80m and 100m are used for the shear estimates. Both data sets have been carefully filtered for faulty data such as icing and for wake directions from operating turbines. Only relatively infrequent wind sectors are influenced by wakes, approximately 340° to 20° for Høvsøre and 30° to 70° as well as 160° to 200° for Ryningsnäs. For consistency with the proposed method the MOL measurements and the estimated concurrent normalized shear and turbulence data are both smoothed as described in 'step 3' of the proposed method (cf. section 3). Finally, to ensure similar appearance of the plots only data for one year is included for each mast, although multiple years are available for Høvsøre. No further filtering has been performed except excluding data for wind speeds below 3m/s. The results of this validation analysis are shown in Figure 5.

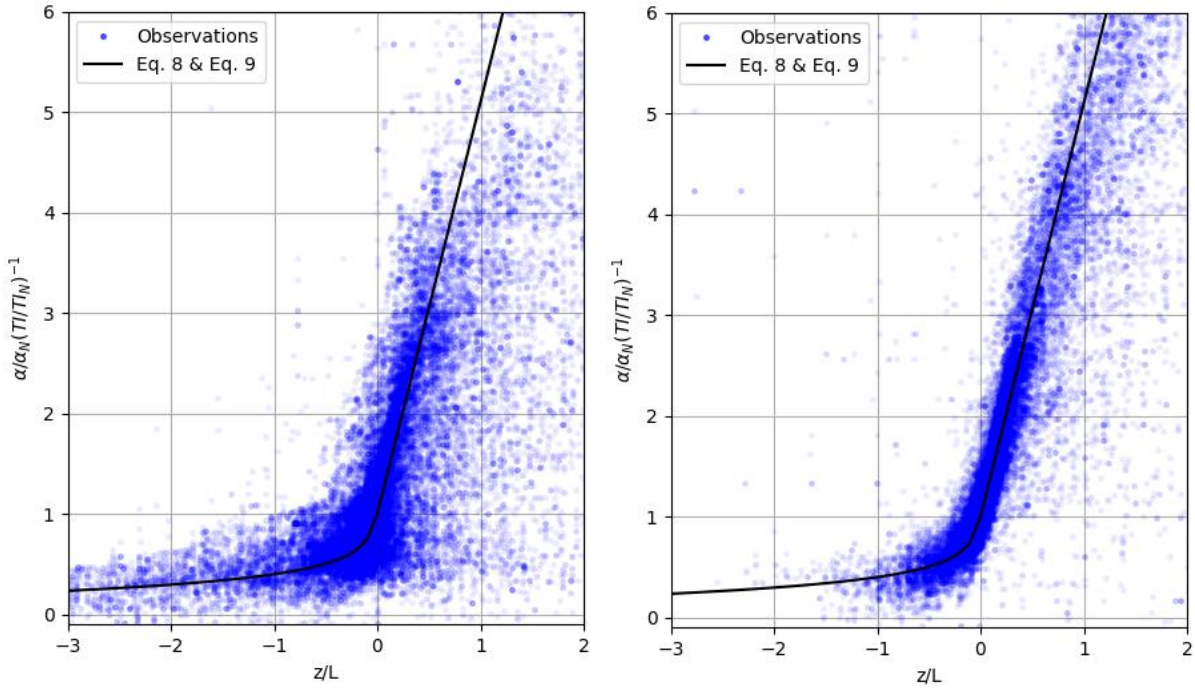

Figure 5. *Validation analysis for the main assumption of the proposed method using data from two research masts, left: Høvsøre (Danish west coast) and right: Ryningsnäs (forested site in southern Sweden). The theoretically derived expressions eq. (8) and (9) are superimposed as the black curve.*

Note the relatively high consistency between the approximate expression and the observed data points of z/L versus $\alpha/\alpha_N\,(TI/TI_N)^{-1}$. The data points in Figure 5 clearly follow the tendency of the superimposed black curve from the equations 8 and 9, which approximate the main assumption of the proposed method, equation (6). For Ryningsnäs there are very few data for $z/L < -1$, indicating that significantly unstable conditions are rare on this forested site. Høvsøre on the other hand has more data representing unstable conditions, and these scatter nicely around the theoretical expectation. In general, the observed scatter can to some degree be explained by the uncertain nature of the measurements. The MOL data are based on 3D-sonic covariances which estimate the heatflux and friction velocity and is a relatively noisy point-measurement itself. Similarly, shear estimates are calculated from wind speed measurements across multiple heights and is often prone to spurious variation and accumulation of error across the sensors. Or the upper shear height may be above ABL in very stable conditions. Furthermore, wind speed trends present within some of the 10min data samples (i.e. non-stationarity) will introduce a bias in the turbulence data. Considering these multiple and significant error sources the main assumption of the proposed method appears to hold surprisingly well for the two analysed masts, clearly reproducing the theoretically derived expressions in equations 8 and 9.

6. Conclusions, recommendations and discussion

This paper presents a novel method to quantify atmospheric stability using measurements from wind power masts with standard instrumentation. The method quantifies stability effects via normalizing observed shear and turbulence by their neutral levels, estimated as the high wind speed limit in each wind direction. A theoretical basis for the proposed method has been established using similarity theory, and describes how the ratio of normalized shear and turbulence only depends on z/L, i.e stability, and is independent of roughness and wind speed. Hence, a ratio of normalized shear and turbulence can be directly converted to a Monin-Obukhov length using the derived universal relationship (equation 6) which itself is a function of universal similarity functions for momentum and turbulence. This universal relationship is approximately linear for the stable part and log-linear for the unstable part. Convenient approximations have been derived (equations 8 and 9) which allow estimation of Monin-Obukhov lengths directly from observed ratios of normalized shear and turbulence.

The method has been demonstrated on data from the Cabauw tower in the Netherlands situated in almost homogenous terrain. The results quite closely resemble the theoretical expectations, but show some scatter which is related to the accumulated uncertainties in the measurements and the limitations of the Monin-Obukhov similarity theory, the basis of the proposed method. The method inherits the limitations of MOST, but this paper presents solid arguments why the use of ratios of the universal functions is less sensitive to the particular constants in the adopted similarity expressions and only requires the similarity expressions to be accurate in a relative sense. Similarly, the ratios of normalized shear and turbulence are less sensitive to potential biases from complex meteorological effects like the Charnock effect for water surfaces. However, the approximate expressions in equation (8) and (9) are based on equation (2) estimating wind shear at a single point of the main height. Using multiple heights for the shear estimate will introduce a small bias relative to this assumption as shown in Figure 1 (right). Thus, it is recommended not to base the shear estimate on heights too far from the main height, contrary to common practice in wind energy applications seeking to estimate the full rotor shear.

The validity of the main assumption of the method, the universal relationship approximated by equation (8) and (9) is tested using measured values of Monin-Obukhov lengths at two research masts in a coastal setting and in a forest. The results of the validation analysis show that the main assumption of the proposed method appears to hold well for the two analysed masts at 80m above ground.

Further validation of the proposed method against measured Monin-Obukhov lengths from 3D-sonics is required, in particular for masts in complex terrain and for multiple measuring levels. This will allow a better understanding of the limitations of the method and test the generality of the approximations in equations (8) and (9).

Acknowledgements
This work is part of the windPROSPER and InnoWind projects, funded by the national Innovation Fund Denmark. Cabauw data are provided via the Cesar data portal and data for DTU masts Høvsøre and Ryningnäs are available via the Rodeo data portal. The authors are very grateful for the support and data contributions.

References

[1] Wagner R, Courtney M, Larsen T J and Paulsen U S 2010 *Simulation of shear and turbulence impact on wind turbine performance* vol Risø-R-172
[2] Newman J and Klein P 2014 The Impacts of Atmospheric Stability on the Accuracy of Wind Speed Extrapolation Methods *Resources* **3** 81–105
[3] Holtslag M C, Bierbooms W A A M and Van Bussel G J W 2014 Estimating atmospheric stability from observations and correcting wind shear models accordingly *J. Phys. Conf. Ser.* **555** 1–10
[4] Kelly M, Larsen G, Dimitrov N K and Natarajan A 2014 Probabilistic meteorological characterization for turbine loads *J. Phys. Conf. Ser.* **524**
[5] Dimitrov N, Natarajan A and Kelly M 2014 Model of wind shear conditional on turbulence and its impact on wind turbine loads *Wind Energy* **17** 657–69
[6] Archer C L, Colle B A, Veron D L, Veron F and Sienkiewicz M J 2016 On the predominance of unstable atmospheric conditions in the marine boundary layer offshore of the U.S. northeastern coast *J. Geophys. Res.* **121** 8869–85
[7] Wharton S and Lundquist J K 2012 Assessing atmospheric stability and its impacts on rotor-disk wind characteristics at an onshore wind farm *Wind Energy* **15** 525–46
[8] Stull R B 1988 *An Introduction to Boundary Layer Meteorology.* (Dordrecht: Kluwer Academic Publishers)
[9] Kaimal J C and Finnigan J J 1994 *Atmospheric Boundary Layer Flows - Their Structure and Measurement* (New York: Oxford University Press)
[10] Panofsky H A and Dutton J A 1984 *Atmospheric Turbulence - Models and Methods for Engineering Applications* (New York: John Wiley & Sons)
[11] Brooks I M, Söderberg S and Tjernström M 2003 The turbulence structure of the stable atmospheric boundary layer around a coastal headland: Aircraft observations and modelling results *Boundary-Layer Meteorol.* **107** 531–59
[12] Pahlow M, Parlange M B and Portè-Agel F 2001 On Monin- Obukhov similarity in the stable atmospheric boundary layer *Boundary-Layer Meterology* **99** 225–48
[13] Park M S and Park S U 2006 Effects of topographical slope angle and atmospheric stratification on surface-layer turbulence *Boundary-Layer Meteorol.* **118** 613–33
[14] Højstrup J 1982 Velocity Spectra in the Unstable Planetary Boundary Layer *J. Atmos. Sci.* **39** 2239–48
[15] Nadeau D F, Pardyjak E R, Higgins C W and Parlange M B 2013 Similarity Scaling Over a Steep Alpine Slope *Boundary-Layer Meteorol.* **147** 401–19
[16] Monna W A A and Van Der Vliet J G 1987 *Facilities for research and weather observations on the 213 m tower at Cabauw and at remote locations. KNMI Scientific Rep. WR-87-5*
[17] Peña A, Floors R, Sathe A, Gryning S E, Wagner R, Courtney M S, Larsén X G, Hahmann A N and Hasager C B 2016 Ten Years of Boundary-Layer and Wind-Power Meteorology at Høvsøre, Denmark *Boundary-Layer Meteorol.*
[18] Arnqvist J, Segalini A, Dellwik E and Bergström H 2015 Wind Statistics from a Forested Landscape *Boundary-Layer Meteorol.* **156** 53–71